differentiation and proliferation of LN cells. TREM2 is a unique molecule that is only expressed on microglia, osteoclasts and immature dendritic cells (Colonna, 2003), while other microglia-specific markers such as Iba1 and CD11b are also expressed on macrophages and monocytes. Because TREM2 was not expressed on the mature dendritic cells or the activated microglia (macrophages), it is likely that TREM2 expression may be restricted to the immature stages of myeloid lineage cells. In our study, M-CSF induced the proliferation of LN cells, and the expression of not only CD11b and Iba1 but also TREM2 on LN cells; this indicates that M-CSF determines the differentiation of LN cells into the myeloid lineage, but not into fully differentiated cells. Although the addition of anti-M-CSF antibodies appears not to suppress the expression of TREM2 on the LN cells, these TREM2+ cells may have originated from more mature precursors that are independent of M-CSF. These immature LN cells would eventually be fully differentiated under physiological conditions. When LN cells were cultured with M-CSF, the number of small round cells in the culture was considerably low, indicating that the small round morphology of the immature cells is not maintained in the presence of only M-CSF. On the other hand, when LN cells were grown in the presence of other glial cells (especially astrocytes), the small round cells were maintained at a concentration of approximately 30% of the total population. Therefore, cell–cell contact with glial cells, especially astrocytes, may be necessary to maintain the small round shape of immature cells expressing TREM2.

Acknowledgements

This research was partially supported by the Ministry of Education, Science, Sports and Culture, Grant-in-Aid for Young Scientists (B), 18790590, 2006 and Contribution to an excellent research project in Multiple Sclerosis, Japanese branch of multiple sclerosis society, 2006 to K.T.

Abbreviations

ERK, extracellular signaling-regulated kinases; FITC, fluorescein isothiocyanate; GFAP, glial fibrillary acidic protein; GFP, green fluorescence protein; LN cells, lineage-negative bone marrow cells; M-CSF, macrophage colony stimulating factor; MHC, major histocompatibility complex; PE, phycoerythrin; TNF-α, tumor necrosis factor-α; TREM2, triggering receptor expressing on myeloid cells-2; VEGF, vascular endothelial growth factor.

References

Akiyama, H. & McGeer, P.L. (2004) Specificity of mechanisms for plaque removal after A beta immunotherapy for Alzheimer disease. *Nat. Med.*, **10**, 117–118; author reply 118–119.

Banati, R.B. (2003) Neuropathological imaging: *in vivo* detection of glial activation as a measure of disease and adaptive change in the brain. *Br. Med. Bull.*, **65**, 121–131.

Colonna, M. (2003) TREMs in the immune system and beyond. *Nat. Rev. Immunol.*, **3**, 445–453.

Fife, B.T., Huffnagle, G.B., Kuziel, W.A. & Karpus, W.J. (2000) CC chemokine receptor 2 is critical for induction of experimental autoimmune encephalomyelitis. *J. Exp. Med.*, **192**, 899–905.

Getts, D.R., Terry, R.L., Getts, M.T., Müller, M., Rana, S., Shrestha, B., Radford, J., Van Rooijen, N., Campbell, I.L. & King, N.J.C. (2008) Ly6c+ "inflammatory monocytes" are microglial precursors recruited in a pathogenic manner in West Nile virus encephalitis. *J. Exp. Med.*, **205**, 2319–2337.

Hänninen, A., Jaakkola, I., Salmi, M., Simell, O. & Jalkanen, S. (1997) Ly-6C regulates endothelial adhesion and homing of CD8(+) T cells by activating integrin-dependent adhesion pathways. *Proc. Natl. Acad. Sci. USA*, **94**, 6898–6903.

Hickey, W.F. & Kimura, H. (1988) Perivascular microglial cells of the CNS are bone marrow-derived and present antigen *in vivo*. *Science*, **239**, 290–292.

Izikson, L., Klein, R.S., Charo, I.F., Weiner, H.L. & Luster, A.D. (2000) Resistance to experimental autoimmune encephalomyelitis in mice lacking the CC chemokine receptor (CCR)2. *J. Exp. Med.*, **192**, 1075–1080.

Kuwabara, Y., Yokoyama, A., Yang, L., Toku, K., Mori, K., Takeda, I., Shigekawa, T., Zhang, B., Maeda, N., Sakanaka, M. & Tanaka, J. (2003) Two populations of microglial cells isolated from rat primary mixed glial cultures. *J. Neurosci. Res.*, **73**, 22–30.

Ling, E.A. & Wong, W.C. (1993) The origin and nature of ramified and amoeboid microglia: a historical review and current concepts. *Glia*, **7**, 9–18.

Mildner, A., Schmidt, H., Nitsche, M., Merkler, D., Hanisch, U.K., Mack, M., Heikenwalder, M., Brück, W., Priller, J. & Prinz, M. (2007) Microglia in the adult brain arise from Ly-6ChiCCR2+ monocytes only under defined host conditions. *Nat. Neurosci.*, **10**, 1544–1553.

Neumann, H. & Takahashi, K. (2007) Essential role of the microglial triggering receptor expressed on myeloid cells-2 (TREM2) for central nervous tissue immune homeostasis. *J. Neuroimmunol.*, **184**, 92–99.

Priller, J., Flügel, A., Wehner, T., Boentert, M., Haas, C.A., Prinz, M., Fernández-Klett, F., Prass, K., Bechmann, I., de Boer, B.A., Frotscher, M., Kreutzberg, G.W., Persons, D.A. & Dirnagl, U. (2001) Targeting gene-modified hematopoietic cells to the central nervous system: use of green fluorescent protein uncovers microglial engraftment. *Nat. Med.*, **7**, 1356–1361.

del Rio-Hortega, P. (1932) Microglia. In Penfield, W.. (ed), *Cytology and Cellular Pathology of the Nervous System*, **vol. 2**. Hoeber, New York, pp. 481–534.

Sanders, P. & De Keyser, J. (2007) Janus faces of microglia in multiple sclerosis. *Brain. Res. Rev.*, **54**, 274–285.

Santambrogio, L., Belyanskaya, S.L., Fischer, F.R., Cipriani, B., Brosnan, C.F., Ricciardi-Castagnoli, P., Stern, L.J., Strominger, J.L. & Riese, R. (2001) Developmental plasticity of CNS microglia. *Proc. Natl. Acad. Sci. USA*, **98**, 6295–6300.

Saura, J., Tusell, J.M. & Serratosa, J. (2003) High-yield isolation of murine microglia by mild trypsinization. *Glia*, **44**, 183–189.

Schmid, C.D., Sautkulis, L.N., Danielson, P.E., Cooper, J., Hasel, K.W., Hilbush, B.S., Sutcliffe, J.G. & Carson, M.J. (2002) Heterogeneous expression of the triggering receptor expressed on myeloid cells-2 on adult murine microglia. *J. Neurochem.*, **83**, 1309–1320.

Servet-Delprat, C., Arnaud, S., Jurdic, P., Nataf, S., Grasset, M.F., Soulas, C., Domenget, C., Destaing, O., Rivollier, A., Perret, M., Dumontel, C., Hanau, D., Gilmore, G., Belin, M.F., Rabourdin-Combe, C. & Mouchiroud, G. (2002) Flt3+ macrophage precursors commit sequentially to osteoclasts, dendritic cells and microglia. *BMC Immunol.*, **3**, 15.

Sessa, G., Podini, P., Mariani, M., Meroni, A., Spreafico, R., Sinigaglia, F., Colonna, M., Panina, P. & Meldolesi, J. (2004) Distribution and signaling of TREM2/DAP12, the receptor system mutated in human polycystic lipomembraneous osteodysplasia with sclerosing leukoencephalopathy dementia. *Eur. J. Neurosci.*, **20**, 2617–2628.

Simard, A.R. & Rivest, S. (2004) Bone marrow stem cells have the ability to populate the entire central nervous system into fully differentiated parenchymal microglia. *FASEB J.*, **18**, 998–1000.

Stefano, L., Racchetti, G., Bianco, F., Passini, N., Gupta, R.S., Bordignon, P.P. & Meldolesi, J. (2009) The surface-exposed chaperone, Hsp60, is an agonist of the microglial TREM2 receptor. *J. Neurochem.*, **110**, 284–294.

Takahashi, K., Rochford, C.D.P. & Neumann, H. (2005) Clearance of apoptotic neurons without inflammation by microglial triggering receptor expressed on myeloid cells-2. *J. Exp. Med.*, **201**, 647–657.

Takahashi, K., Prinz, M., Stagi, M., Chechneva, O. & Neumann, H. (2007) TREM2-transduced myeloid precursors mediate nervous tissue debris clearance and facilitate recovery in an animal model of multiple sclerosis. *PLoS Med.*, **4**, e124.

Tanaka, J., Toku, K., Sakanaka, M. & Maeda, N. (1999) Morphological differentiation of microglial cells in culture: involvement of insoluble factors derived from astrocytes. *Neurosci. Res.*, **34**, 207–215.

Vaughan, D.W. & Peters, A. (1974) Neuroglial cells in the cerebral cortex of rats from young adulthood to old age: an electron microscope study. *J. Neurocytol.*, **3**, 405–429.

Wang, C.C., Wu, C.H., Shieh, J.Y., Wen, C.Y. & Ling, E.A. (1996) Immunohistochemical study of amoeboid microglial cells in fetal rat brain. *J. Anat.*, **189** (Pt 3), 567–574.

Neuroradiology
DOI 10.1007/s00234-010-0684-7

DIAGNOSTIC NEURORADIOLOGY

Brachial and lumbar plexuses in chronic inflammatory demyelinating polyradiculoneuropathy: MRI assessment including apparent diffusion coefficient

Yuko Adachi · Noriko Sato · Tomoko Okamoto · Masayuki Sasaki · Hirofumi Komaki · Fumio Yamashita · Jiro Kida · Tomoyuki Takahashi · Hiroshi Matsuda

Received: 21 December 2009 / Accepted: 11 March 2010

Abstract
Introduction Our purpose was to clarify the magnetic resonance (MR) imaging characteristics of the brachial and lumbar plexuses in patients with chronic inflammatory demyelinating polyradiculoneuropathy (CIDP) using various kinds of sequences, including diffusion-weighted images (DWI).
Methods We evaluated the MR imaging findings for lumbar and/or brachial nerve plexuses in 13 CIDP patients and 11 normal volunteers. The nerve swelling was evaluated in comparison with normal controls by coronal short tau inversion recovery (STIR), and signal abnormalities were evaluated by coronal STIR, T1-weighted images, and DWIs. The degrees of contrast enhancement and apparent diffusion coefficient (ADC) values of the plexus were also assessed.
Results In the patient group, diffuse enlargement and abnormally high signals were detected in 16 out of 24 plexuses (66.7%) on STIR, a slightly high signal was detected in 12 of 24 plexuses (50%) on T1-weighted images, and a high-intensity signal was detected in 10 of 18 plexuses (55.6%) on DWIs with high ADC values. Contrast enhancement of the plexuses was revealed in 6 of 19 plexuses (31.6%) and was mild in all cases. There were statistically significant differences between the ADC values of patients with either swelling or abnormal signals and those of both normal volunteers and patients without neither swelling nor abnormal signals. There were no relationships between MR imaging and any clinical findings.
Conclusion STIR is sufficient to assist clinicians in diagnosing CIDP. T1-weighted images and DWIs seemed useful for speculating about the pathological changes in swollen plexuses in CIDP patients.

Keywords Chronic inflammatory demyelinating polyradiculoneuropathy · Peripheral nerve · Diffusion-weighted MRI · Apparent diffusion coefficient · Onion bulb

Y. Adachi · N. Sato (✉) · F. Yamashita · J. Kida · T. Takahashi
Department of Radiology,
National Center Hospital of Neurology and Psychiatry,
4-1-1 Ogawahigashi-cyo,
Kodaira, Tokyo 187-8511, Japan
e-mail: snoriko@ncnp.go.jp

T. Okamoto
Department of Neurology,
National Center Hospital of Neurology and Psychiatry,
4-1-1 Ogawahigashi-cho,
Kodaira, Tokyo 287-8511, Japan

M. Sasaki · H. Komaki
Department of Child Neurology,
National Center Hospital of Neurology and Psychiatry,
4-1-1 Ogawahigashi-cho,
Kodaira, Tokyo 287-8511, Japan

H. Matsuda
Department of Nuclear Medicine,
Saitama Medial University Hospital,
38 Morohongo, Moroyama-cho,
Iruma-gun, Saitama 350-0495, Japan

Published online: 20 April 2010

Introduction

Chronic inflammatory demyelinating polyradiculoneuropathy (CIDP) is an acquired peripheral neuropathy of presumed autoimmune etiology, which is either a chronically progressive or relapsing–remitting disorder [1]. The

major symptoms are bilateral proximal and distal limb muscle weakness and sensory loss. Motor deficits are usually predominant. This disease commonly affects brachial or lumbar plexuses distributed in the muscles of the extremities. Cranial or diaphragmatic nerve involvement is rarely seen. The involved peripheral nerves in CIDP reveal a unique pathological finding. They are grossly enlarged due to proliferation of surrounding Schwann cells, causing an "onion bulb" appearance [1], although the axons are usually preserved.

A diagnosis of CIDP is generally based on clinical features and electrophysiological studies. As the disease has been studied in various clinical trials, several clinical definitions of this neuropathy have been proposed [2–4]. Cerebrospinal fluid examination, nerve biopsy, and magnetic resonance (MR) examinations provide supportive information but are not always required for diagnosis. However, demonstrable MR imaging findings have been reported, and they are helpful for diagnosis.

Several studies have described the MR imaging findings of CIDP patients. Swelling brachial or lumbar plexuses with increased signal intensity on T2-weighted images with or without contrast enhancement have been reported [5–9]. Coronal short tau inversion recovery (STIR) imaging is particularly helpful for depicting the signal abnormalities of brachial and lumbar plexuses [6]. However, no original reports have evaluated either the diffusion property in patients with CIDP or the T1-weighted images obtained before gadolinium administration, although the contrast enhancement pattern of the nerve plexus has been examined [5, 6].

In this study, we evaluated MR imaging findings of the brachial or lumbar plexus in patients with CIDP using STIR, T1-weighted images before and after contrast enhancement, and diffusion-weighted MRI (DWI), along with the calculation of apparent diffusion coefficient (ADC) values. The aim of this study was to demonstrate the MR imaging findings including some new sequences and to clarify the role of the MR examination in supporting the diagnosis of CIDP.

Materials and methods

Patients

The subjects included 13 consecutive patients (five males and eight females, ranging in age from 5 to 85 years old, mean age±SD; 45.2±25.0 years) who consulted our hospital from 2004 to 2007 and agreed to undergo an MR imaging examination. MR images of all 13 patients with CIDP were retrospectively reviewed. The patients all met the clinical and neurophysiological criteria for CIDP (Joint Task Force of the EFNS and PNS) [2]. No other cause of the neuropathy was found in clinical, laboratory, or histological investigations. None of the patients had a history of exposure to neurotoxic agents or a family history of neuropathy. Disease duration at the time of the MR studies ranged from 6 months to 20 years (mean±SD; 5.0± 6.2 years). Eleven patients had the relapsing–remitting form of the disease and two had the progressive form (cases 3 and 7). In eight patients, no treatment was administered before the MR study. In two patients (cases 1 and 4), immunoglobulin was administered before the MR examination because Guillain–Barre syndrome had been one of their possible diagnoses. The remaining three patients (cases 5, 8, and 10) had long disease duration, and both immunoglobulin and corticosteroid therapy had already been administered before the MR studies. The F wave, which indicated motor conduction along the entire peripheral axon including the radicular segment, was examined as an electrodiagnostic study in all patients. The median nerve conduction was measured at the wrist, and the tibial nerve conduction was measured at the ankle. In one patient, a biopsy was performed at the sural nerve with pathological confirmation of CIDP.

MR studies were also performed in 11 normal volunteers (six males and five females) as a control group. Their ages ranged from 22 to 73 years (mean±SD; 56.5±16.7 years). This study had appropriate Ethics Committee approval.

Imaging

MR examinations were performed on a 1.0-T scanner (Harmony; Siemens, Erlangen, Germany) using a spine array coil. MR studies of both cervical and lumbar plexuses were acquired in all but two (cases 4 and 8) of the 13 patients. One of these two (case 8) underwent an MR examination of only the brachial plexuses, and the other underwent that (case 4) of only the lumbar plexus. In total, 24 nerve plexuses in thirteen patients were evaluated. Coronal STIR and fat-saturated T1-weighted images were acquired in all studies. Gadolinium was administered in all but three patients (cases 8, 10, and 11). One patient (case 4) underwent gadolinium administration only in the MR examination of the brachial plexus, not in the study of the lumbar plexus. The other patients underwent gadolinium administration in MR studies of both the brachial and lumbar plexuses. In total, gadolinium was administered in the examinations of 19 nerve plexuses in 10 patients. DWIs were not acquired in four patients (cases 4, 5, 6, and 8), and thus DWIs were obtained in examinations of 18 nerve plexuses in nine patients.

Follow-up MR studies were carried out in two patients. One patient (case 9) underwent MR studies three times over 8 months: before treatment, after treatment, and during the

relapse phase. In another patient (case 1), a follow-up MR study was performed 1 year after the first study, although he had no clinical symptoms.

Among the 11 normal volunteers, MR studies of both the cervical and lumbar plexuses were carried out in two cases, of only the brachial plexus in five cases, and of only the lumbar plexus in four cases. In total, 13 plexuses were evaluated. Coronal STIR, fat-saturated T1-weighted images, and DWIs were obtained in all normal volunteers. Gadolinium administration was not performed.

The parameters of the coronal STIR sequence were as follows: repetition time/echo time/inversion time [TR/TE/TI], 4,210/85/150; 4-mm sections without gaps; fields of view [FOV], 260×260 (brachial plexus), 280×280 (lumbar plexus); imaging matrix, 512×512; number of excitations (NEX), 1. The parameters of the coronal fat-saturated T1-weighted image sequence before and after gadolinium administration were [TR/TE]=1,330/16; 3-mm sections without gaps; FOV, 260×260 (brachial plexus), 280×280 (lumbar plexus); imaging matrix, 512×512, NEX, 2. The DWIs were obtained using an axial single-shot spin-echo echo-planar imaging sequence with the following parameters: [TR/TE/TI], 10,000.0/86.0/150; 4-mm sections without gaps; FOV, 400×400 (brachial and lumbar plexus); imaging matrix, 256×256; and NEX, 3. Motion-probing gradients were applied in six directions (*xx*, *yy*, *zz*, *xy*, *xz*, and *yz*) with *b* values of 0 and 1,000 s/mm^2. The scan time was 8 min and 20 s in the brachial plexus and 7 min and 40 s in the lumbar plexus. We then performed maximum intensity projection (MIP) for a stack of isotropic DWIs to reconstruct the images rotated around the *z*-axis using software incorporated into the MR system. The isotropic DWIs were generated based on calculated isotropic ADC values.

Image analysis

Imaging assessment in the patient group was based on agreement between two neuroradiologists who reviewed the images in tandem and who were blinded to clinical information regarding neuropathies. Each neuroradiologist made initial evaluations independently, and any disagreements regarding the final conclusion were resolved by consensus.

Swelling of the plexuses was visually assessed on STIR in comparison to the controls. The signal intensity of each plexus was also evaluated on both STIR and T1-weighted images without contrast enhancement and compared to the signal intensity of the controls. We also visually assessed the signal intensity of the plexus on T1-weighted images after contrast enhancement and compared it to the intensity on images taken before contrast enhancement. We established a grading system for the degree of enhancement in the plexuses: moderate enhancement means that the plexuses have stronger enhancement than the ganglions, and mild enhancement means that the plexuses have milder enhancement than the ganglions. DWIs (b=1000) with MIP reconstruction along the long axis of the spine were also assessed by comparison with the controls.

We measured the ADC values of the plexuses on ADC maps. All of the ADC measurements were made using an Aquarius Netstation Ver 1.4 (Tera Recon, San Mateo, CA, USA) by placing freehand circular regions of interest (ROIs) over the plexus on the ADC map. The average ROI was 4±2 mm^2, and the area varied depending on the plexus. ROIs were carefully placed by two trained operators within the plexus to avoid the partial volume effect at three points, and the ADC values were averaged in each lesion. The intra-class correlation coefficient for these measurements was 92.0%. Intra-class correlation coefficient values greater than 0.9 were regarded as excellent, and the results were thus considered reliable. The differences in the ADC values of the plexuses among healthy subjects, patients without neither swelling nor abnormal signals of the plexus, and patients with either swelling or abnormal signals of the plexus were evaluated by analysis of variance. P values less than 0.05 were considered significant.

Using the unpaired t test, we also evaluated the relationships between age at onset and each MR imaging finding, such as nerve swelling, high signal intensity on STIR, T1-weighted images, DWI, and degree of enhancement. Disease duration was also evaluated in the same way. Additionally, the relationships between each MR finding and the clinical findings (motor and sensory symptoms and F wave latency) were evaluated by Fisher's exact test.

Results

Clinical and imaging features

The clinical and MR imaging findings are summarized in Table 1. All patients presented with motor and/or sensory symptoms in both the upper and lower extremities. F wave latencies were prolonged in either the upper or lower extremities or both of all patients, except for two (cases 2 and 5), whose F waves were absent, probably due to severe nerve damage.

Swelling of the brachial and lumbar plexuses was observed in 16 of 24 plexuses (66.7%) on STIR in 9 out of 13 CIDP patients (Figs. 1 and 2). In the patients who underwent both brachial and lumbar MR examinations, either both plexuses were simultaneously swollen or neither was swollen.

High intensity was shown in 16 of 24 plexuses (66.7%) on STIR in 9 out of 13 CIDP patients, and all 16 plexuses were swollen (Fig. 1a). Slightly high intensity was found in

Table 1 Comparison of clinical and MR imaging findings in patients with CIDP.

Case	Age/sex	Clinical findings					MR findings					
		Disease duration (years)	Portion	Motor symptoms	Sensory symptoms	F wave latencies	Swelling of plexus	High intensity on STIR	High intensity on T1-WI	CE	High intensity of DWI	ADC value ($\times 10^{-3}$ mm^2/s)
1	13/M	0.5	B	+	−	Prolonged	+	+	+	−	+	1.91
			L	+	+	Prolonged	+	+	+	−	+	1.96
2	16/F	6	B	+	−	NR	+	+	+	−	+	1.69
			L	+	−	NR	+	+	+	−	+	2.12
3	39/M	4	B	+	+	Prolonged	+	+	+	−	+	1.43
			L	+	−	Normal	+	+	+	−	+	1.26
4	5/F	1	B	+	−	Normal	Not done	Not done	Not done	Not done	Not done	Not done
			L	+	+	Prolonged	+	+	−	−	Not done	Not done
5	46/M	17	B	+	+	NR	+	+	−	+	Not done	Not done
			L	+	+	NR	+	+	−	+	Not done	Not done
6	64/M	3	B	+	−	Prolonged	+	+	+	−	Not done	Not done
			L	+	+	Normal	+	+	+	−	Not done	Not done
7	66/M	2	B	+	−	Prolonged	+	+	+	+	+	1.50
			L	+	+	Normal	+	+	+	+	+	1.18
8	67/F	20	B	+	−	Prolonged	+	+	−	Not done	Not done	Not done
			L	+	−	Prolonged	Not done	Not done	Not done	Not done	Not done	Not done
9	34/M	1	B	+	+	Prolonged	+	+	+	+	+	1.43
			L	+	−	Prolonged	+	+	+	+	+	1.20
10	85/F	10	B	+	+	Normal	−	−	−	Not done	−	0.98
			L	+	−	Prolonged	−	−	−	Not done	−	1.04
11	36/F	2	B	+	+	Prolonged	−	−	−	Not done	−	0.73
			L	+	+	Normal	−	−	−	Not done	−	0.92
12	75/F	4	B	+	−	Prolonged	−	−	−	−	−	0.78
			L	+	−	Prolonged	−	−	−	−	−	0.77
13	42/F	4	B	−	+	Normal	−	−	−	−	−	0.89
			L	−	+	Prolonged	−	−	−	−	−	1.05

Upper extremity normal F wave latency <32 ms; lower extremity normal F wave latency <60 ms; NR = no response due to absent distal F wave

M male, *F* female, *B* brachial plexus, *L* lumbar plexus, *STIR* short tau inversion recovery, *WI* weighted image, *CE* contrast enhancement, *DWI* diffusion-weighted image, *ADC* apparent diffusion coefficient

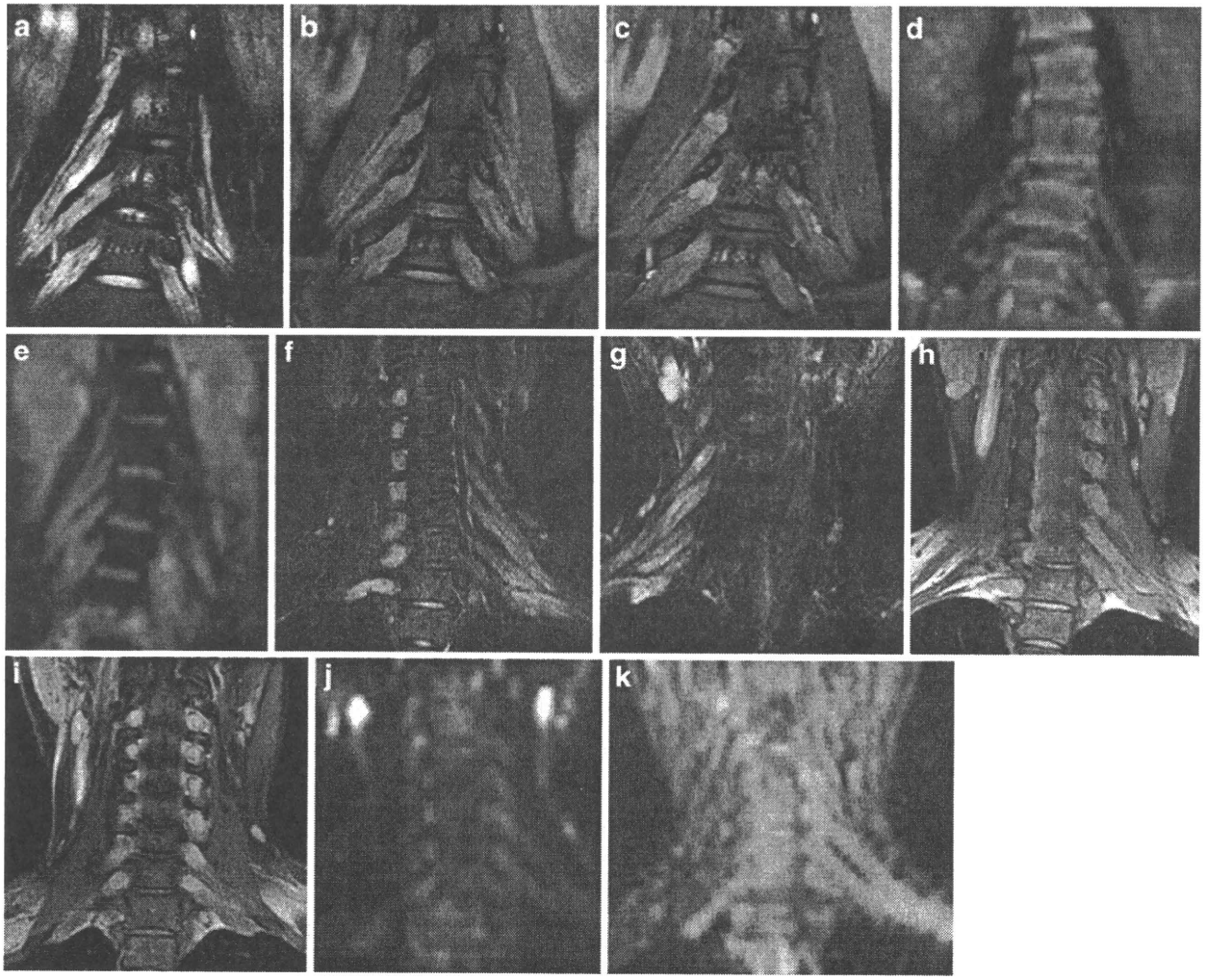

Fig. 1 MR images of a 16-year-old female (case 2 in Table 1) with chronic inflammatory demyelinating polyradiculoneuropathy (CIDP) with symmetrical weakness of both legs and arms for 5 years. **a** Coronal STIR image of the lumbar plexus shows enlargement with a markedly high signal. **b** Lumbar plexus with hypertrophy shows slightly high signal intensity on T1-weighted images without contrast enhancement. **c** T1-weighted images following intravenous gadolinium administration shows an enhancement in the nerve ganglion without enhancement of the lumbar plexus. **d** DWI reconstructed by MIP on the lumbar plexus shows high intensity of the lumbar plexus. **e** ADC map of the lumbar plexus. The ADC value in the lumbar plexus with hypertrophy was $2.1\times10^{-3}mm^3/s$. **f, g** Coronal STIR reveals hyperintensity and swelling of the bilateral brachial plexus (because this patient had torticollis, both plexuses do not appear in the same slice). **h** Brachial plexus with hypertrophy shows slightly high signal intensity on T1-weighted images. **i** T1-weighted images following intravenous gadolinium administration do not show contrast enhancement of the nerve plexus. **j** DWI demonstrates high signal intensity. **k** The mean ADC value in the brachial plexus was $1.7\times10^{-3}mm^3/s$

12 of 24 plexuses (50%) on T1-weighted images without contrast enhancement in six patients (Fig. 1b).

Contrast enhancement was shown in 6 of 19 plexuses (31.6%) in 3 out of 10 patients after gadolinium administration (Fig. 2c). All enhanced plexuses showed mild enhancement. In patients who underwent MR studies of both the brachial and lumbar plexuses, either both plexuses were simultaneously enhanced, or neither was enhanced. All enhanced plexuses showed swelling and hyperintensity on STIR.

On DWIs, high intensity was found in 10 of 18 plexuses in 5 out of 9 patients (55.6%); all 10 plexuses showed swelling and high intensity on STIR and slightly high intensity on T1-weighted images before gadolinium administration (Fig. 1a, b, e). The remaining eight plexuses that did not show high intensity on DWIs did not show swelling or high intensity on STIR or on T1-weighted images.

In one patient who was examined three times in total from before to after treatment (case 9), all MR findings such as swelling, signals in all sequences, and contrast

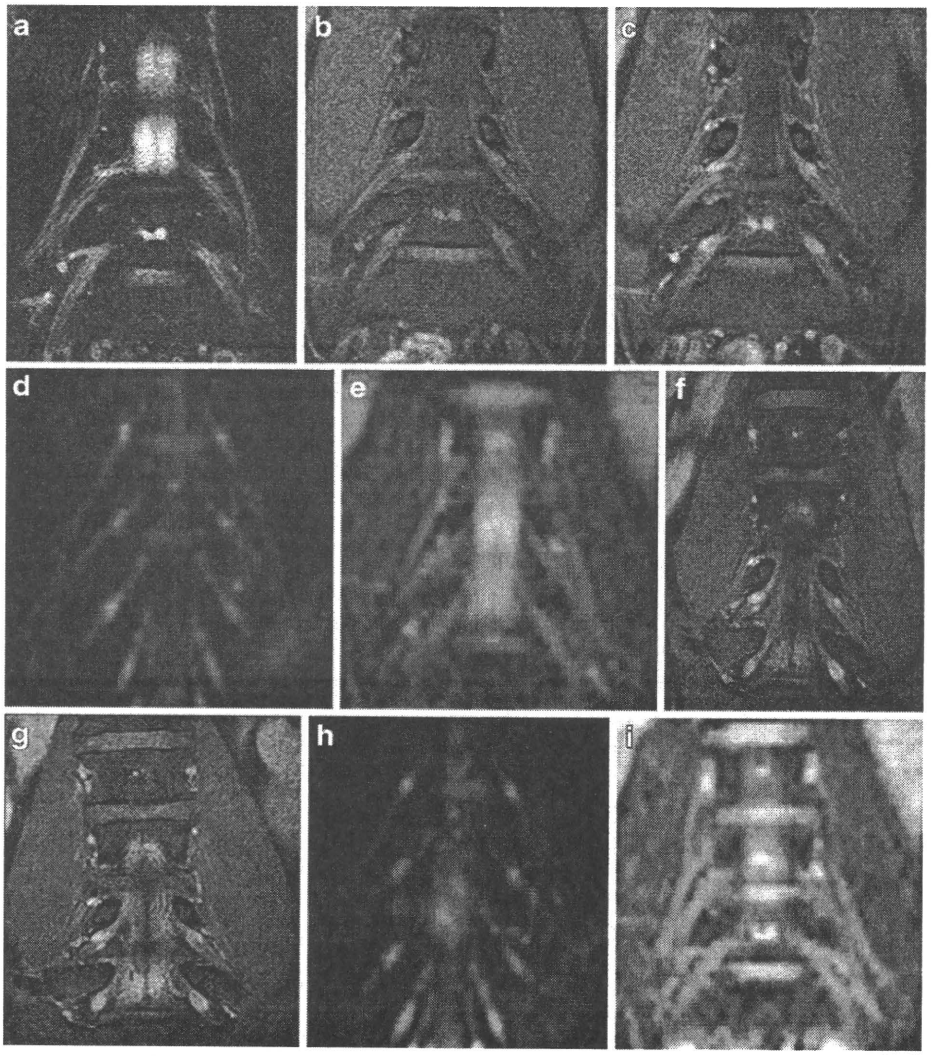

Fig. 2 MR images from a 34-year-old man (case 9 in Table 1) with CIDP, with a 6-month history of weakness in both legs and arms as well as sensory loss in the arms. **a** Coronal STIR image reveals moderate swelling and hyperintensity of the lumbar plexus bilaterally. **b** Lumbar plexus with hypertrophy shows slightly high signal intensity on T1-weighted image. **c** T1-weighted image following intravenous gadolinium administration shows mild enhancement in the lumbar plexus. **d** DWI reconstructed by MIP on the lumbar plexus demonstrates high intensity. **e** ADC map of the lumbar plexus. The ADC value was 1.5×10^{-3} mm^3/s. **f** T1-weighted images with gadolinium obtained 1 month after immunoglobulin therapy; the degree of enhancement is unchanged. **g** T1-weighted image with gadolinium obtained at the relapse phase, 6 months after immunoglobulin therapy; the degree of enhancement is unchanged. **h** DWI reconstructed by MIP on the lumbar plexus after treatment obtained at the same time as **g** shows no remarkable changes in the intensity of the lumbar plexus. **i** ADC map of the lumbar plexus. The ADC value was $1.5\times10^{-3}mm^3/s$

enhancement remained unchanged throughout the examinations without interval changes even during the remission phase or relapse phase (Fig. 2c, f, g). Another follow-up study in case 1 also showed no interval changes.

Swollen plexuses were not observed in any of the 11 normal volunteers. All of their plexuses showed isointensity or faintly high intensity on both STIR and T1-weighted images (Fig. 3).

Among the patients, no significant relationships were observed between MR images and clinical findings.

Measurements of ADC values

The mean ADC values in the plexuses of patients and normal volunteers were $1.27\pm0.43\times10^{-3}mm^2/s$ (n=18) and $0.92\pm0.11\times10^{-3}mm^2/s$ (n=13), respectively. The mean ADC values in patients with and without both swelling and high intensity of the brachial/lumbar plexus on STIR were $1.56\pm0.34\times10^{-3}mm^2/s$ (n=10) and $0.89\pm0.12\times10^{-3}mm^2/s$ (n=8), respectively. There were statistically significant differences between the ADC values of the patients with either swelling or abnormal signals and both normal volunteers and patients without neither swelling nor abnormal signals. However, there was no significant difference in ADC values between patients without neither swelling nor abnormal signals and normal volunteers.

Discussion

The diagnosis of CIDP is based mainly on the clinical presentation and on nerve conduction findings that are consistent with demyelination. However, in clinical practice, CIDP is often difficult to diagnose. MR examination of the brachial and lumbar plexuses will be very helpful in diagnosing CIDP.

In the present study, the MR imaging findings for nerve plexuses in CIDP patients were examined using various

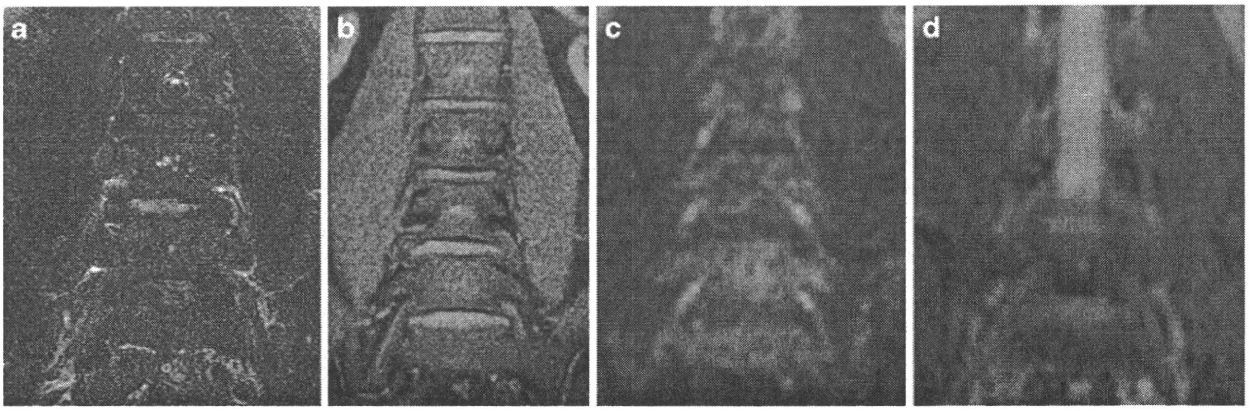

Fig. 3 MR images of a 64-year-old normal male volunteer. **a** Coronal STIR image shows the lumbar plexus without swelling or abnormal high intensity. **b** T1-weighted image shows the lumbar plexus with isointensity except for the proximal portion. **c** DWI reconstructed by MIP depicts the lumbar plexus faintly at the proximal portion. **d** The ADC value of the lumbar plexus was 1.1×10^{-3}mm^3/s

kinds of sequences, including T1-weighted images and DWIs, which had not previously been evaluated in a large number of CIDP patients. Although the most sensitive sequence for detecting signal abnormalities was STIR, T1-weighted images and DWI sequences also detected approximately 50% of the abnormalities. Moreover, high intensities on both DWI and the ADC map, which are indicative of T2 shine-through, may reflect a pathological condition in which the nerve plexus is shaped like an onion bulb.

There have been several MR studies of CIDP, some of which have shown diffuse brachial and lumbar plexus swelling and high signal intensity on T2-weighted images or STIR [5–8]. In one study, hypertrophy on MR images of plexuses in CIDP was observed in 57.1% of patients; this result is slightly lower than, but relatively consistent with the frequency observed in our study. If swelling and increased signal intensity can be detected on STIR in the plexuses of patients with clinically suspected CIDP, these findings will be of diagnostic value [6, 8].

DWIs have been investigated in several previous attempts to visualize extraspinal neural structures [10–12]. In one recent study, the quality of depiction of the brachial plexus on DWIs was evaluated [12]. The study involved five volunteers, three patients with cervical schwannoma, and two with traumatic lesions of the brachial plexus. Their study showed that DWI reconstructed by MIP provided an overview image of the brachial plexus. However, no ADC values were calculated, and the lumbar plexus was not included. Tsuchiya et al. have described the nerve roots and peripheral nerves in patients with various diseases, including three cases with CIDP, six with multiple sclerosis, and four with neurogenic tumors, using DWI [11]. They showed the affected lesion in the cord and proximal nerve roots clearly on DWI, which suggested that the DW sequence would have the potential to visualize the intramedullary and nerve root lesions, and thus facilitating a differential diagnosis. However, these studies examined several kinds of peripheral nerve diseases and included only a few CIDP cases. In addition, the ADC values were not obtained in these studies. Thus far, there have been no original MR studies with DWIs focusing on CIDP patients, nor have any studies evaluated normal brachial or lumbar plexuses on DWIs with ADC values. However, several studies have examined DWIs of normal peripheral nerves [13, 14] and have shown the normal ADC value of the median nerve to be $1.01\pm0.13\times10^{-3}$mm^2/s. Our study also demonstrated similar ADC values of the brachial and lumbar plexuses (mean $0.92\pm0.11\times10^{-3}$mm^2/s) in normal volunteers.

In this study, the DWIs showed a high signal in 55.6% of the plexuses of CIDP patients; thus, DWIs would be helpful for detecting abnormal nerve plexuses. Furthermore, patients with plexus hypertrophy had significantly higher mean ADC values than patients without hypertrophy or in the normal volunteers. Thus, the high intensity of swollen plexuses on DWIs was attributed to the T2 shine-through effect. In a study by Crino et al., the swelling of the nerve plexuses of CIDP patients was found to be caused by several proliferating layers of Schwann cells around the axon, which increased endoneurial collagen [15]. These pathological changes would explain the increased ADC values within the hypertrophic nerves. The ADC values of Schwann cell cytoplasm and endoneurial collagen surrounding bare axons in CIDP patients may be higher than those for normal myelin with tight junctions.

T1-weighted images before contrast enhancement have rarely been evaluated in CIDP patients. This study showed slightly high signal intensity in the brachial and lumbar plexuses on T1-weighted images in 50% of patients with

CIDP. During the process of re-myelination of peripheral nerves in CIDP patients, the plexus gradually becomes brighter on T1-weighted images, probably reflecting the development of the onion bulb and increased endoneurial collagen [16]. Additionally, in the course of demyelination and re-myelination, phagocytic macrophages of myelin debris are increased. Some of the lipids taken up by Schwann cells may be used to supply cholesterol for rapid membrane biogenesis by macrophages, in order to prepare for the formation of neuritis [17]. We speculate that these conditions shorten the T1 of the plexus in CIDP patients.

In the peripheral nerves of CIDP patients, increased permeability of the blood–nerve barrier appears to be the cause of spinal roots and plexus enhancement. Gadolinium enhancement has been reported in some, but not all cases of CIDP [5, 8, 10]. Midroni et al. detected the enhancement of the nerve root and the extraforaminal segment in 28.6% of cases, which was slightly lower than the 31.6% frequency observed in the present study. There has been no agreement regarding whether the enhancement of peripheral nerves indicates disease activity [7, 9]. In one of our patients who showed clinical improvement after treatment, the mild enhancement remained unchanged from before to after the treatment.

The differential diagnoses of CIDP are Charcot–Marie–Tooth (CMT) disease, distal demyelinating polyneuropathy associated with monoclonal gammopathy, and multifocal motor neuropathy (MMN). Swelling and increasing intensity on STIR with or without enhancement in nerve plexuses have also been noted in patients with distal demyelinating polyneuropathy associated with monoclonal gammopathy [5]. CMT disease, which is a hereditary peripheral neuropathy, also mimics MR findings of CIDP [18]. Because recurrent demyelination and re-myelination occur in CMT disease, the peripheral nerves often show an onion bulb as in CIDP [16]. MMN is characterized by asymmetric weakness without sensory loss. Usually, MR abnormalities are detected asymmetrically in MMN but symmetrically in CMT disease, CIDP, and distal demyelinating polyneuropathy associated with monoclonal gammopathy [19]. In particular, the affected nerve areas in CMT disease are more diffuse than in the other conditions.

Our study has several limitations. First, 12 of the 13 patients met the clinical and neurophysiological criteria for CIDP without nerve biopsy. Furthermore, in the pathologically confirmed patient, a biopsy was performed at the sural nerve and not at the plexus itself, because a biopsy at the lumbar nerve plexus carries some risks and is not usually done for the purpose of diagnosis. Although the obtained DWIs and ADC values were useful for speculating about the pathological changes in nerve plexuses in CIDP, they were not conclusive. Second, we had one follow-up study of gadolinium administration (case 9), and two follow-up studies on DWIs (cases 1 and 9). Both studies revealed no interval changes, even though one patient showed improved clinical symptoms (case 1). We think it is important for clinicians to know that there is no definite relationship between the response to treatment and any MR findings. The lack of interval changes suggests that once an onion bulb has formed, it is rarely resorbed by treatment. However, follow-up was carried out in only two patients, and a longer-term follow-up study on more patients needs to be performed.

Conclusions

Although the standard method for diagnosing CIDP includes the evaluation of clinical features and electrophysiological examinations, characteristic MR findings on STIR in CIDP patients are found to be helpful in making a diagnosis. In particular, DWIs and T1-weighted images without contrast enhancement seem useful for speculating about the pathological changes in swollen plexuses in CIDP patients.

No definite relationship was observed between MR imaging findings and clinical findings.

Conflict of interest statement We declare that we have no conflict of interest.

References

1. Hahn A, Hartung H, Dick P (2005) Chronic inflammatory demyelinating polyradiculoneuropathy. In: Dick P (ed) Peripheral neuropathy, vol 2, 4th ed. Elsevier, Philadelphia, pp 2221–2253
2. Joint Task Force of the EFNS and the PNS (2005) European Federation of Neurological Societies/Peripheral Nerve Society Guideline on management of chronic inflammatory demyelinating polyradiculoneuropathy: report of a joint task force of the European Federation of Neurological Societies and the Peripheral Nerve Society. J Peripher Nerv Syst 10:220–228
3. Latov N (2002) Diagnosis of CIDP. Neurology 59(Suppl 6):S2–S6
4. Koller H, Kieseier BC, Jander S, Hartung HP (2005) Chronic inflammatory demyelinating polyneuropathy. N Engl J Med 352:1343–1356
5. Eurelings M, Notermans NC, Franssen H, Van Es H, Ramos H, Wokke J, Van Den Berg H (2001) MRI of the brachial plexus in polyneuropathy associated with monoclonal gammopathy. Muscle Nerve 24:1312–1318
6. Bradley L, Wilhelm T, King RH, Ginsberg L, Orrell RW (2006) Brachial plexus hypertrophy in chronic inflammatory demyelinating polyradiculoneuropathy. Neuromuscul Disord 16:126–131
7. Midroni G, Tilly TN, Gray B, Vajsar J (1999) MRI of the cauda equine in CIDP: clinical correlations. J Neurol Sci 170:36–44
8. Duggins A, McLeod J, Pollard J, Davies L, Yang F, Thompson EO, Soper JR (1999) Spinal root and plexus hypertrophy in

chronic inflammatory demyelinating polyneuropathy. Brain 122:1383–1390
9. Kuwabara S, Nakajima M, Matsuda S, Hattori T (1997) Magnetic resonance imaging at the demyelinative foci in chronic inflammatory demyelinating polyneuropathy. Neurology 48:874–877
10. Tsuchiya K, Imai M, Tateishi H, Nitatori T, Fujikawa A, Takemoto S (2007) Neurography of the spinal nerve roots by diffusion tensor scanning applying motion-probing gradients in six directions. Magn Reson Med Sci 6:1–5
11. Tsuchiya K, Honya K, Yoshida M, Nitatori T (2008) Demonstration of spinal cord and nerve root abnormalities by diffusion neurography. J Comput Assist Tomogr 32:286–290
12. Takahara T, Hendrikse J, Yamashita T, Mali W, Kwee T, Imai Y, Luijten P (2008) Diffusion-weighted MR neurography of the brachial plexus: feasibility study. Radiology 249(2):653–660
13. Bendszus M, Stoll G (2005) Technology insight: visualizing peripheral nerve injury using MRI. Nat Clin Pract Neurol 1:45–53
14. Kababci N, Gurses B, Firat Z. Bayram A, Ulug A, Kovanlikaya A (2007) Diffusion tensor imaging and tractography of median nerve: Normative diffusion values. AJR 189:923–927
15. Crino B, Grossman I, Rostami A (1993) Magnetic resonance imaging of the cauda equine in chronic inflammatory demyelinating polyneuropathy. Ann Neurol 33:311–313
16. Graham I, Lantos L (2002) Greenfield's neuropathology, 7th edition, Vol. 2. New York Oxford University Press, pp 617–620
17. Naba I, Yoshikawa H, Sakoda S, Itabe H, Suzuki H, Kodama T, Yanagihara T (2000) Onion-bulb formation after a single compression injury in the macrophage scavenger receptor knockout mice. Exp Neurol 166:83–89
18. Sureka J, Charian RA, Alexander M, Thomas BP (2009) MRI of brachial plexopathies. Clin Radiol 64:208–218
19. Van Es H, Van den Berg L, Franssen H et al (1997) Magnetic resonance imaging of the brachial plexus in patients with multifocal motor neuropathy. Neurology 48(5):1218–1224

病態と治療

神経疾患と炎症

—多発性硬化症を中心に—

千原典夫*　山村　隆**

要　旨

慢性炎症の役割がさまざまな神経疾患で推察されている．中でも多発性硬化症で代表される免疫性神経疾患では，T細胞やB細胞の介在する炎症病態がかなり詳細に解析されている．神経組織は血液組織関門により保護されているが，一方では神経細胞には十分な自己再生能がなく，その障害機序の解明と治療法の開発にはさまざまな因子を考慮しなければならない．本稿では多発性硬化症を中心に，炎症の介在する神経障害の機序や治療戦略について，最新の知見を紹介する．

はじめに

慢性炎症の介在する神経疾患の病態では，神経組織が血液脳関門（blood–brain barrier）や血液神経関門（blood–nerve barrier）に守られていること，神経系で免疫機能を担うグリア細胞が他の臓器の免疫担当細胞とは異なる性質を示すこと，および神経変性過程が十分に理解されていないことなどに配慮する必要がある．本稿では代表的な慢性炎症性神経疾患として多発性硬化症（MS）を取り上げ，最近の知見を解説する．

* 国立精神・神経医療研究センター 神経研究所 免疫研究部
** 同 部長

キーワード：多発性硬化症（MS），抗原特異的T細胞，ミクログリア，血液脳関門，神経変性

多発性硬化症（MS）

MS は中枢神経内に多発性の炎症性病変を生じる疾患で，若年の女性に発症する傾向が強い．臨床的には永年にわたって再発と寛解を繰り返すが，徐々に神経変性が進行して車椅子生活を余儀なくされるケースもまれではない．我が国の患者数は 30 年前には 1,000 人程度であったが，現在では 12,000 人以上に増加し，近年の増加傾向が明らかである．MS は中枢神経系髄鞘に由来するミエリン抗原（ミエリン塩基性タンパク質など）に反応するT細胞やB細胞が関与する自己免疫疾患である．

1．MS の病態に関する新しいモデル

1）病変の始まり

MS の病変は脳室周囲，深部大脳白質，大脳皮質などに散在し，その大きさは顕微鏡で

ようやく観察できるレベルから，小指大，こぶし大までさまざまである．個々の病変の形成過程に関してはいまだ明らかでない部分が多いが，神経病理学の専門家は最近，初期の軽微な組織破壊と，それに引き続いて起こるミエリン抗原特異的T細胞の活性化による髄鞘破壊の2ステップに分けて考えることを提唱している（図1）[1]．

従来はT細胞浸潤および髄鞘崩壊が最も早期の病理的な変化とされていたが，2004年にPrineasらは，ミクログリアの活性化を伴うオリゴデンドロサイトのアポトーシス様細胞死が，髄鞘の崩壊する前に起こったと判断せざるを得ない症例を報告し，議論を巻き起こした[2]．彼らの論文では，炎症細胞は血管周囲には認められたが，病変部にはほとんど存在しなかった．病変はたとえるなら，低酸素によって惹起される組織破壊像（脳梗塞病変）に極めて類似していた．興味あることに，同じような組織破壊像を示したMS病変において，他の研究者はミクログリアに発現した一酸化窒素合成酵素（iNOS）やミエロペルオキシダーゼ（MPO）を介したNOや活性酸素産生によってミトコンドリア障害が生じる可能性を指摘した[3]．これらの病理学的な観察に基づいて，MSの病変は，まず血管周囲の炎症性細胞などから何らかの炎症性物質が中枢神経系内で放出され，その間接的作用によってミクログリアが過剰に活性化し，オリゴデンドロサイトのミトコンドリア障害を誘導して初期病変を作り，それに続いて破壊されたミエリン断片に反応した抗原特異的T細胞の活性化と大規模の髄鞘破壊が生じるという2ステップモデルが提唱されている．しかし，ミクログリアを活性化する原因はほかにもフィブリン，Toll-like receptor（TLR）のリガンド，感染など諸説あり，このモデルの妥当性についてはさらなる検証が必要と思われる．

2．血液脳関門に関する研究の進歩

血液脳関門が存在するために，末梢で活性化された炎症細胞は中枢神経系の実質に容易には侵入することができない．血液脳関門は血管内皮とグリア境界膜（glia limitans）の2層構造からなり，グリア境界膜はアストロサイトの足突起と基底膜から構成される．炎症細胞が血管から血液脳関門を越えて中枢神経系に侵入する過程は，血流の中で血管内皮に接着し血管外のperivascular space（概念的にはくも膜下腔と同義）へ侵入する過程と，グリア境界膜を破壊して中枢神経実質に侵入する過程に分けられる．最初の過程ではリンパ球が血管内皮に接着するプロセスが必須であり，その際にはT細胞の発現する接着分子$\alpha_4\beta_1$インテグリン（VLA-4）と血管内皮の発現するVCAM-1の相互作用が重要である[4]．また後の過程では，T細胞やその他の炎症細胞によって産生されるサイトカインやマトリックスメタロプロテアーゼが決定的な役割を果たす[5]．

近年Bartholomäusらは，二光子励起顕微鏡を用いて髄膜血管表面を移動するT細胞を観察し，ミエリン抗原特異的T細胞のみならず，中枢神経内には存在しない抗原（卵白アルブミン）に特異的なT細胞も血管内からくも膜下腔へ遊走することを示した．この結果は，活性化T細胞であれば，抗原特異性には関係なく血管外へ遊走することを意味する[6]．しかし，ミエリン抗原特異的T細胞だけがグリア境界膜を越え，卵白アルブミン特異的T細胞は越えなかった．この理由として，ミエリン抗原特異的T細胞はくも膜下腔においてミエリン抗原によって再度活性化され，サイトカインやケモカインを産生するのに対して，卵白アルブミン特異的T細胞は抗原がないため再活性化されないからであることが分かった．実際，卵白アルブミンを人為的にくも膜下腔に添加すると，卵白アルブミン特異的T

図1 多発性硬化症（MS）病態の概念図

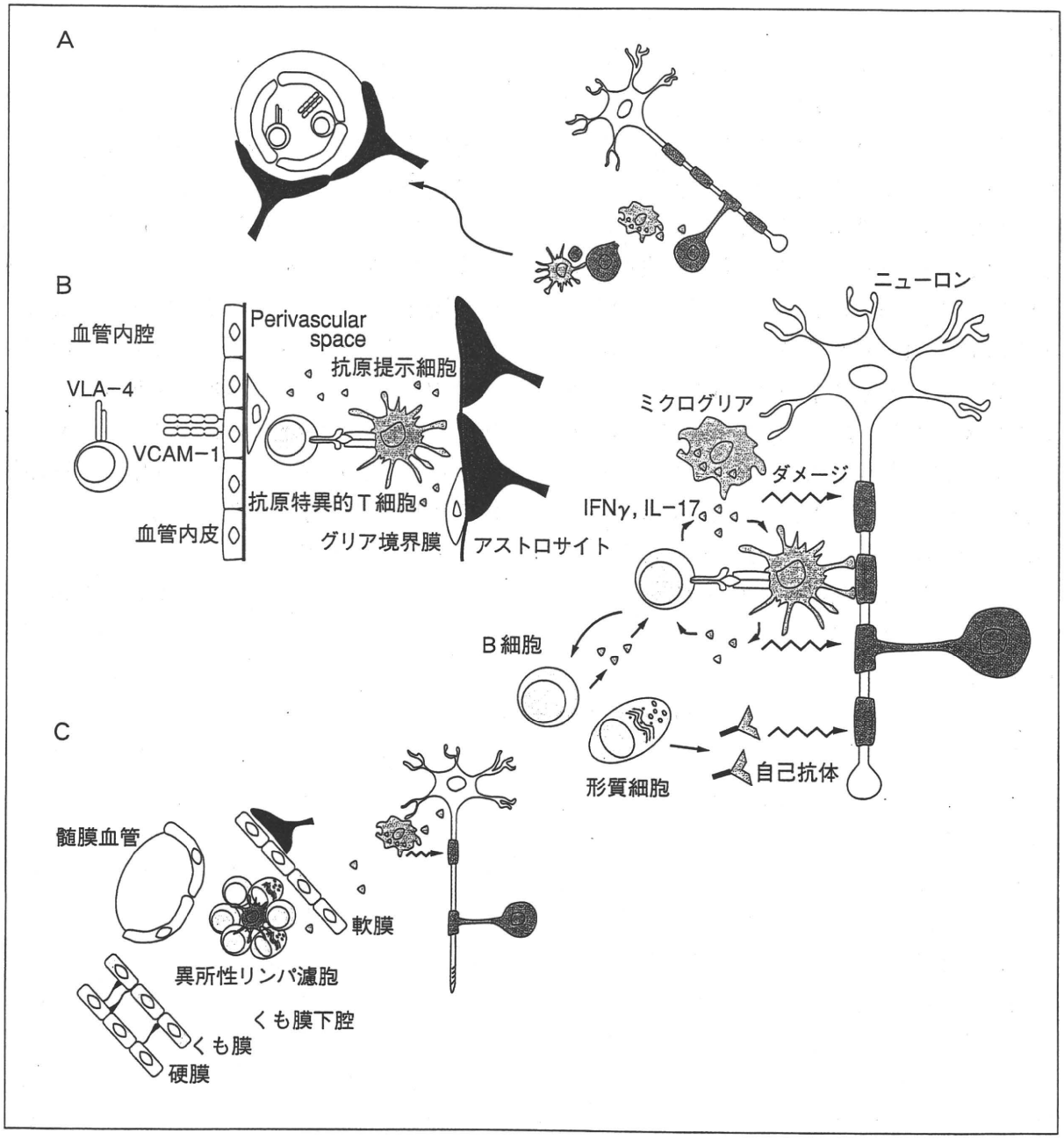

A：病変の始まり．ミクログリアによるオリゴデンドロサイトの障害で髄鞘タンパク質が細胞外へ溶出し，抗原提示細胞に貪食される．

B：初期病変．Perivascular space に浸潤した抗原特異的T細胞は，髄鞘タンパク質の提示を受けて再活性化し，中枢神経へと浸潤する．抗原特異的T細胞は，B細胞，マクロファージなどが介在する炎症の司令塔となり，髄鞘障害，神経障害を惹起する．

C：進行期病変．くも膜下腔に形成された異所性リンパ濾胞などに刺激を受けたミクログリアによる髄鞘，軸索障害が続く．

略語：巻末の「今月の略語」参照

細胞もグリア境界膜を越えることが証明された．

3．治療に関する話題

1）インターフェロン（IFN）療法

ヘルパーT（Th）細胞はT細胞，B細胞，

マクロファージなどがかかわる獲得免疫の司令塔をつかさどっている．炎症を惹起するThとしてはTh1細胞とTh17細胞の存在が知られていたが，最近ではIL-9を産生するTh9細胞も炎症を惹起することが報告されている[7]．一方，炎症を調節・抑制する細胞として，Th2細胞，制御性T細胞，NKT細胞などが知られている．現在，慢性期のMSに対する維持療法として，国内で使用できる薬剤はIFNβに限られているが，IFNβの薬効としてはTh1細胞とTh2細胞のバランスを調整する機能などが知られている．しかし約半数の患者では有効性が認められず，特定の病態に対してはむしろ増悪させる可能性が示唆されてきた．最近，MSの動物モデルである実験的自己免疫性脳脊髄炎（EAE）を用いてIFNβの薬効メカニズムについて解析され，Th1細胞で誘導したEAEにはIFNβが有効であるが，Th17細胞で誘導したEAEではIFNβ投与によって逆に症状の増悪が見られることが報告された[8]．さらにMS患者末梢血を用いた解析により，IFN療法に反応しない患者では治療前にTh17の産生するIL-17Fの血中濃度が高いことも示された．一連の解析結果は，MSの病態においてTh1細胞が病態形成に重要な場合とTh17細胞が重要な場合が存在し，前者にはIFNβ治療が有効であるが，後者ではむしろ病態を悪化させてしまう可能性を示唆している．

近年になって，従来MSと診断されていた症例の中から，グリア境界膜を形成するアストロサイトの足突起に高発現するアクアポリン4（AQP4）に対する自己抗体が検出されることが分かった．このような症例は視神経脊髄炎（NMO）の臨床病型をとるものに多く，MSとは区別してNMO spectrum disorder（NMOSD）と診断されるようになった．抗AQP4抗体はそれ自体がアストロサイト障害活性を有し，抗AQP4抗体陽性の症例は通常のMSとは異なる[9]．IFNβ治療は抗体産生を促進し，NMOSDを悪化させることがあるので，NMOSDにはIFNβを処方しないことが推奨されている．NMOSDは視神経・脊髄に炎症を繰り返す患者が多いが，中には通常のMSのように大脳病変を主体とするものもある．したがって臨床的にMSと診断されている場合でも，必ず抗AQP4抗体が陰性であることを確認してから治療方針を立てる必要がある．なお，NMOではIL-17タンパク質濃度が上昇することが報告されており[10]，IFNβ治療によるNMOSDの悪化はNMOSDにおけるTh17細胞の役割を意味している可能性がある．

2）その他の治療

現在，MSに対する分子標的療法の検討が進んでいる．病変へのリンパ球の輸送を標的とした治療として，抗VLA-4抗体療法（ナタリズマブ）はT細胞の血管内皮への接着を阻止して中枢神経へのリンパ球浸潤を防ぐ．S1P1受容体に結合してリンパ節からのリンパ球の遊走を防ぐ薬剤FTY720（フィンゴリモド）も，MSの再発抑制効果を示した[11]．リンパ球自体を標的とした治療としては，B細胞を標的とした抗CD20抗体（リツキシマブ）によるB細胞の除去療法がMSの再発を防ぐことが証明されている[12]．抗CD20抗体でB細胞を除去したマウスでは，ミエリン抗原による刺激を行っても抗原提示が十分になされず，抗原特異的なTh1細胞やTh17細胞の分化が抑制されEAEが軽快した[13]．このことから，リツキシマブは主にB細胞による抗原提示機能を抑制することによって効果を発揮するようである．成熟リンパ球，単球細胞や樹状細胞を標的とした抗CD52抗体（アレムツズマブ）の再発抑制効果も報告されている．アレムツズマブは，末梢のリンパ球に神経保護因子であるBDNFやPDGFの発現を誘導し，*in vitro*ではオリゴデンド

図2 多発性硬化症（MS）病態の変化

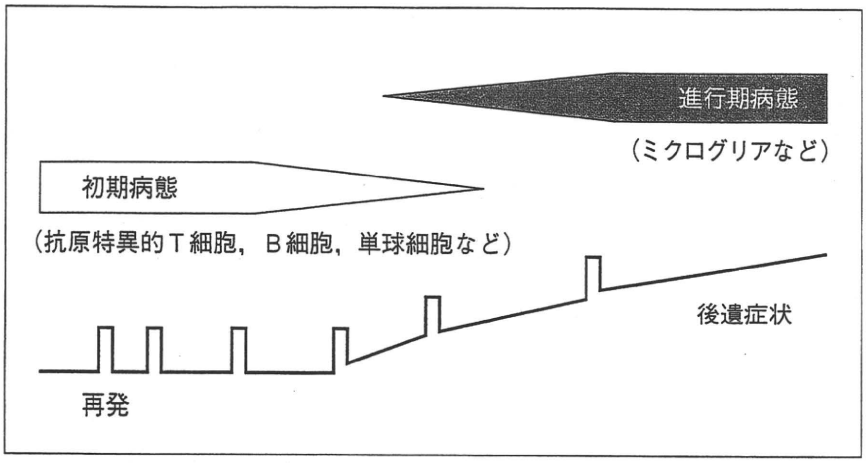

再発・寛解を繰り返す初期病態から，徐々に神経脱落症状が蓄積する進行期病態に移行する．初期はT細胞やB細胞を主とする獲得免疫が，進行期にはミクログリアなどの自然免疫が炎症の中心となる．

ロサイトの前駆細胞の生存や髄鞘形成を促進する．したがって，神経保護にもかかわっている可能性がある[14]．

4．神経変性と炎症

抗炎症療法は発症早期の炎症病態に対する効果は得られるが，慢性期に緩徐進行する神経症状に対する効果は限定的である．さまざまな臨床的あるいは病理学的な解析によって，MS の初期には炎症病態が主体であるが，進行期には神経変性過程が主体になるとされてきた（図2）[15]．しかし詳細に観察すると，神経変性の進行している病変部位ではミクログリアの活性化が著明であり，自然免疫の関与が示唆されている[16]．

では，なぜ抗炎症療法は MS の進行期においては効果がないのか？ さまざまな可能性が論議されているが，治療に反応しない慢性 MS では，血液脳関門が修復された状態で脳内深部に炎症が持続し，そのために薬剤が病変部位に移行しなくなっている可能性がある．また，髄膜下にリンパ濾胞様の構造物が形成されると[17]，やはり末梢から投与した抗炎症薬が届かなくなる可能性がある．なお，アルツハイマー病や他の神経変性疾患と同様に，MS の進行期病態においても酸化ストレスに伴うミトコンドリア障害の存在が示唆されている．初期病態と異なり，代償性のミトコンドリア数や酵素活性の増加は見られない．

神経変性の過程を明らかにする研究が必要であることは論を待たないが，神経保護や再生を促す治療法も視野に入ってきた．近年では，軸索成長阻害因子である Nogo や髄鞘阻害因子 Lingo-1 に対する阻害療法が，EAE において軸索や髄鞘の再生を促進することが示された[18][19]．現在盛んに行われているモノクローナル抗体療法が進行期にどのような影響を及ぼすかは今後の経過を追う必要があるが，同時に神経変性の抑制や再生を促す治療の発展が待たれる．

おわりに

MS に関する近年のトピックスを中心に病態と治療法について述べてきたが，その自己免疫機序や進行期病態など，いまだ明らかでない部分が多い．患者それぞれの病態に応じたテーラーメード医療を確立するためにも，さらなる研究の進展が求められている．

神経障害を来す慢性炎症性疾患はほかにも，全身性エリテマトーデス，抗リン脂質抗体症

候群，ベーチェット病，サルコイドーシス，慢性炎症性脱髄性神経根炎（CIDP）などがあり，それぞれに特徴的な免疫病態が推測される．MS を role model として，これらの疾患でもさらなる病態の解明と治療法の開発が進むことが期待される．

文　献

1) Lassmann H: What drives disease in multiple sclerosis: inflammation or neurodegeneration? Clin Exp Neuroimmunol 1: 2–11, 2010.
2) Barnett M H, et al: Relapsing and remitting multiple sclerosis: pathology of the newly forming lesion. Ann Neurol 55: 458–468, 2004.
3) Marik C, et al: Lesion genesis in a subset of patients with multiple sclerosis: a role for innate immunity? Brain 130: 2800–2815, 2007.
4) Agrawal S, et al: Dystroglycan is selectively cleaved at the parenchymal basement membrane at sites of leukocyte extravasation in experimental autoimmune encephalomyelitis. J Exp Med 203 (4): 1007–1019, 2006.
5) Ransohoff R M: Natalizumab for multiple sclerosis. N Engl J Med 356: 2622–2629, 2007.
6) Bartholomäus I, et al: Effector T cell interactions with meningeal vascular structures in nascent autoimmune CNS lesions. Nature 462: 94–98, 2009.
7) Dardalhon V, et al: IL–4 inhibits TGF–β–induced Foxp3$^+$ T cells and, together with TGF–β, generates IL–9$^+$IL–10$^+$Foxp3$^-$ effector T cells. Nat Immunol 9 (12): 1347–1355, 2008.
8) Axtell R C, et al: T helper type 1 and 17 cells determine efficacy of interferon–β in multiple sclerosis and experimental encephalomyelitis. Nat Med 16 (4): 406–412, 2010.
9) Wingerchuk D M, et al: The spectrum of neuromyelitis optica. Lancet Neurol 6: 805–815, 2007.
10) Ishizu T, et al: Intrathecal activation of the IL–17/IL–8 axis in opticospinal multiple sclerosis. Brain 128: 988–1002, 2005.
11) Kappos L, et al: A placebo–controlled trial of oral fingolimod in relapsing multiple sclerosis. N Engl J Med 362 (5): 387–401, 2010.
12) Weber S, et al: B–cell activation influences T–cell polarization and outcome of anti–CD20 B–cell depletion in central nervous system autoimmunity. Ann Neurol: 2010. (in press)
13) Hauser S L, et al: B–cell depletion with rituximab in relapsing–remitting multiple sclerosis. N Engl J Med 358 (7): 676–688, 2008.
14) Jones J L, et al: Improvement in disability after alemtuzumab treatment of multiple sclerosis is associated with neuroprotective autoimmunity. Brain 133 (Pt 8): 2232–2247, 2010.
15) Weiner H L: The challenge of multiple sclerosis: how do we cure a chronic heterogeneous disease. Ann Neurol 65: 239–248, 2009.
16) Kutzelnigg A, et al: Cortical demyelination and diffuse white matter injury in multiple sclerosis. Brain 128: 2705–2712, 2005.
17) Magliozzi R, et al: Meningeal B–cell follicles in secondary progressive multiple sclerosis associate with early onset of disease and severe cortical pathology. Brain 130: 1089–1104, 2007.
18) Mi S, et al: LINGO–1 antagonist promotes spinal cord remyelination and axonal integrity in MOG–induced experimental autoimmune encephalomyelitis. Nat Med 13: 1228–1233, 2007.
19) Karnezis T, et al: The neurite outgrowth inhibitor Nogo A is involved in autoimmune–mediated demyelination. Nat Neurosci 7: 736–744, 2004.

Neurological Disorders and Inflammation －From the Aspect of Multiple Sclerosis－

Norio Chihara, Takashi Yamamura
Department of Immunology, National Institute of Neuroscience,
National Center of Neurology and Psychiatry (NCNP)

NKT細胞と多発性硬化症

三宅幸子（国立精神・神経センター神経研究所免疫研究部室長）
山村　隆（国立精神・神経センター神経研究所免疫研究部部長）

Point

- iNKT細胞は、TCRとしてインバリアントなα鎖を発現し、限られたVβ遺伝子と会合するためTCRの可変性が乏しく、またMHC class I類似の多様性のないCD1d分子に提示された糖脂質を抗原として認識する。
- iNKT細胞の機能的な特徴は、TCRを介した刺激によりIL-4、IFN-γを含む多くのサイトカインを短時間で大量に産生することである。
- 自己免疫疾患においてiNKT細胞がどのような機能を果たしているかについては不明であるが、多発性硬化症の寛解期においてiNKT細胞は疾患を抑制するように働いていることが推定される。
- iNKT細胞のリガンドであるα-ガラクトシルセラミドの変異体を用いて、iNKT細胞を標的とした自己免疫疾患治療に注目が集まっている。
- MAIT細胞は第二のインバリアントNKT細胞として注目されている。MHC class I類似のMR1分子が分化に関与し、粘膜に多く存在する。マウスの多発性硬化症モデルでは、病態抑制に関与することが報告されている。

多発性硬化症（multiple sclerosis；MS）は、自己の髄鞘抗原を標的とする自己免疫疾患と考えられている。MSは、一般に再発と寛解を繰り返す疾患であり、その病態の変化には免疫調節細胞の役割が注目されている。

NKT（natural killer T）細胞は、NKマーカーを有するT細胞の総称で、エフェクター作用と免疫抑制作用を合わせもつ多機能性の細胞である。拘束される抗原提示分子や、抗原特異性、抗原を認識するT細胞受容体（TCR）の可変性などによって、いくつかのサブポピュレーションがあることが知られている（**図1**）。そのなかで、CD1拘束性でTCRα鎖に可変性のないinvariant鎖（マウスではVα14Jα18、ヒトではVα24Jα18）を発現するiNKT（invariant NKT）細胞の解析が最も進んでいる[1]。CD1拘束性で通常のTCRを発現する細胞はタイプⅡ NKT細胞とよばれ、iNKT細胞とは異なる性質をもつことが報告されている[2]。MR1（major histocompatibility molecule related 1）拘束性で、invariant鎖（マウスではV1914Jα33、ヒトではVα7.2Jα18）を発現するT細胞も存在し、MAIT（mucosal-associated invariant T）細胞として研究が始まっている[3]。本稿では解析の進んでいるiNKT細胞と最近解析が始まったMAIT細

0910-0474/10/￥400/論文/JCOPY

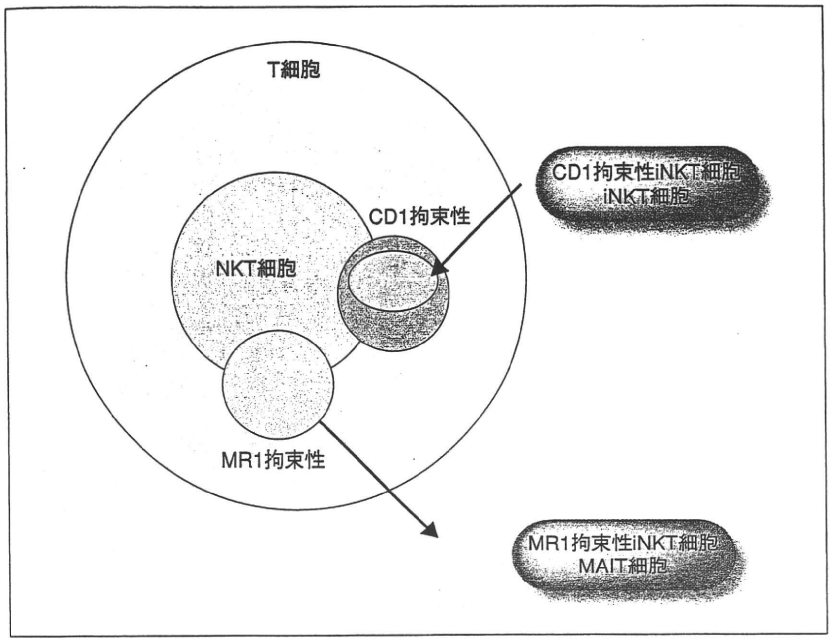

図1　iNKT細胞

NKT細胞は、NKマーカーをもつT細胞の総称である。そのなかで最も解析が進んでいるのは、invariant鎖(マウスではVα14Jα18、ヒトではVα24Jα18)を発現するiNKT細胞である。iNKT細胞は、CD1dによって抗原提示を受ける。CD1d拘束性であって、Vα14Jα18(マウス)もしくはVα24Jα18(ヒト)を発現していない細胞も存在する。Vα14i以外でも、invariant鎖(ヒトではVα7.2α33、マウスではVα19Jα18)を発現するMAIT細胞の存在が知られている。

胞について、基礎的な解説とMSとの関連・それらの細胞を利用した治療法開発について概説する。

iNKT細胞

1. iNKT細胞の特徴：抗原提示分子と抗原

iNKT細胞は、TCRとしてインバリアントなα鎖を発現し、限られたVβ遺伝子(マウスではVβ8.2、Vβ7、Vβ2、ヒトではVβ11)と会合するため、TCRの可変性が乏しく、また主要組織適合遺伝子複合体(major histocompatibility complex；MHC) class Ⅰ類似の多様性のないCD1d分子に提示された糖脂質を抗原として認識するユニークな細胞集団である[1](**図2**)。抗原受容体の可変性に乏しく、クローン性の増殖を必要とせず組織に多数存在してすぐに反応を開始できることなどから、iNKT細胞は自然免疫系と獲得免疫系の中間的存在として、さまざまな免疫の初期応答や調節に関与する。糖脂質を抗原として認識することが特徴であり、微生物などに由来する抗原と、内因性の抗原が報告されている。これまで内因性抗原としては、ガングリオシドGD3、glycosylphosphatidylinositol(GPI)、phosphoethanolamine(PE)などが報告され、最近イソグロボシド(iGb3)が有力な抗原として示されたが、いずれも確定されていない。一方、外来抗原としては、leishmania由来のglycoinositol phospholipids(GIPLs)やlipophosphoglycan(LPG)、sphingomonas由来のglycosphingolipid(GSL)などが報告されている。

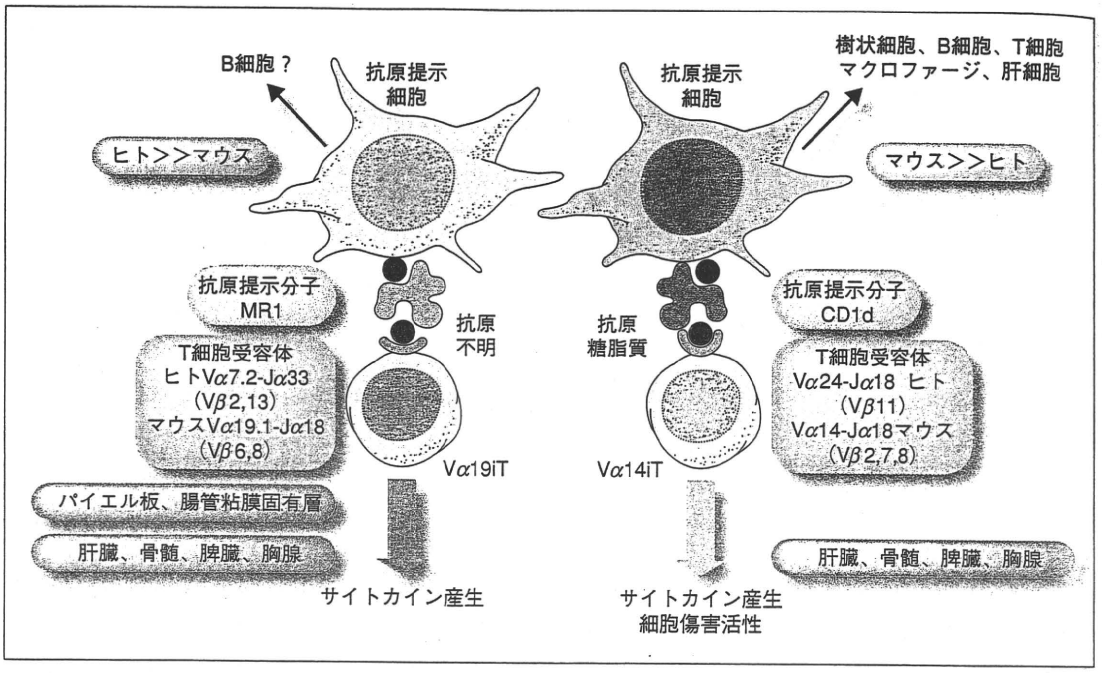

図2　iNKT細胞とMAIT細胞の比較

iNKT細胞は、ヒトではVα24Jα18、マウスではVα14Jα18のinvariant鎖を発現し、CD1dによって提示された糖脂質を抗原として認識する。ヒトではVα7.2α33、マウスではVα19Jα18のinvariant鎖を発現するT細胞は、腸管関連リンパ組織に多く分布することから、mucosal associated invariant T(MAIT)細胞とよばれる。その分化はMR1分子や腸内細菌叢に依存する。iNKT細胞とMAIT細胞は、T細胞受容体の可変性が乏しいことや、Class Ⅰb分子に抗原提示されることなどは類似しているが、ヒトとマウスでの頻度や、細胞の分布については相違がある。

はじめに同定された抗原が合成糖脂質であったことから、これまでiNKT細胞の研究には主にα-ガラクトシルセラミド(α-GC)などの合成糖脂質が用いられてきた。iNKT細胞の機能を研究するだけでなく、α-GCは抗がん剤として治験が進められているほか、α-GCの構造をもとにして、さまざまな糖脂質を合成してiNKT細胞からの特定の機能を強く引き出す糖脂質を探索するという研究も進められている。

2. iNKT細胞の機能的特徴

機能的な特徴としては、TCRを介した刺激によりIL-4、IFN-γを含む多くのサイトカイン(IL-2,-3,-4,-5,-10,-13,17,-21,-22、GM-CSF、TGF-β、オステオポンチン)を短時間で大量に産生することである。iNKT細胞は、マウスに抗CD3抗体を投与すると、数時間後に血中でIL-4の上昇がみられるが、iNKT細胞はその際のIL-4の主要な産生細胞である。細胞あたりのサイトカイン産生能としても、iNKT細胞は*in vitro*で分化させたTh1、Th2細胞に匹敵するIFN-γ、IL-4産生能をもつ。また、IL-17を自身で産生するほか、IL-17を産生するTh17細胞の調節にも関与することが報告されている。iNKT細胞が活性化されると、NK細

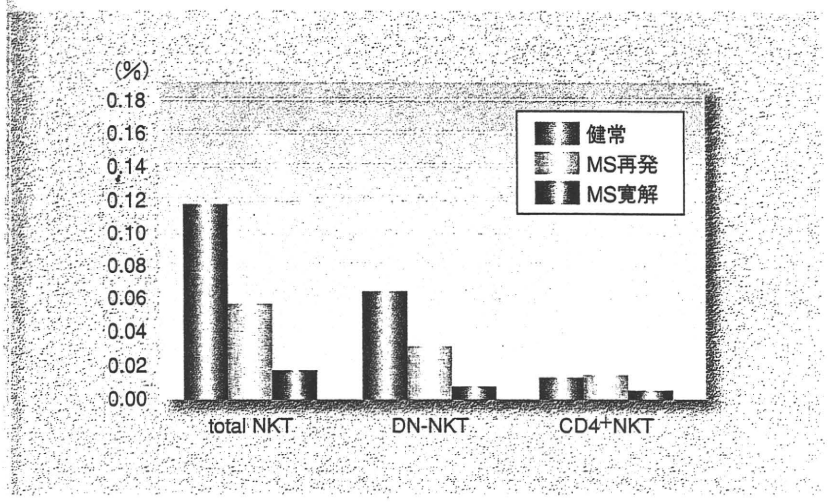

図3　多発性硬化症(MS)患者末梢血における iNKT細胞の頻度

iNKT細胞は、MS寛解期において健常人と比較してその頻度が減少している。MS再発時にはさらに減少している。この減少は、主にdouble negative NKT細胞の減少によると考えられる。

胞でのIFN-γ産生が高まったり、B細胞の活性化マーカーが上昇する、樹状細胞を活性化する、またCD4$^+$CD25$^+$T細胞を介して免疫抑制を行うなど、多くの細胞に影響を与えて免疫反応を修飾する。iNKT細胞は、CD4$^-$CD8$^-$(DN)と、CD4$^+$の細胞があるが、ヒトではDNがマウスではCD4$^+$が多い。特にヒトでは、サブセットによるサイトカイン産生パターンが異なることが示されている。刺激によって、DN-iNKT細胞はIFN-γ、TNF-αといったTh1サイトカインや細胞傷害活性に関与する蛋白を発現するが、CD4陽性細胞はそれらに加えてTh2サイトカインを産生する。生体内でこれらのサイトカイン産生は、状況に応じて調節されているようである。細菌感染などによってIL-12が上昇する環境では、iNKT細胞は外来抗原の刺激が存在しなくともTh1サイトカインを選択的に産生するという報告がある一方、喘息患者の肺胞洗浄液中のiNKT細胞はIL-4やIL-13といったTh2サイトカインを選択的に産生していることが報告されている。また、抗原提示細胞の種類や共刺激の違いによってもiNKT細胞の反応は異なる。樹状細胞がiNKT細胞からTh1、Th2を強く誘導する一方、肝細胞、消化管上皮細胞、皮膚上皮細胞などはTh2サイトカインを弱く誘導する。これらのnon-professionalな抗原提示細胞は共刺激分子を欠くが、professionalな抗原提示細胞でも共刺激を阻害すると同様な効果がみられる。肝臓、消化管、皮膚などは、常に外界からの抗原刺激にさらされるために、過剰な免疫応答による炎症を抑制する機構にiNKT細胞も貢献している可能性が考えられる。

3. 多発性硬化症におけるiNKT細胞

MSでは、寛解期にある患者では、健常人と比較して減少しているが、再発期にはiNKT細胞の減少はむしろ軽度になる。減少しているのはDN-iNKT細胞であり、CD4$^+$iNKT細胞は寛解期、再発時ともに減少していなかった(図3)。サイトカイン産生に関しては、DN-iNKT細胞では寛解期にIL-4、IFN-γともに産生の低下がみられた